JOC Featured Article

pubs.acs.org/joc

Pyrazinacenes: Aza Analogues of Acenes

Gary J. Richards,[†,‡] Jonathan P. Hill,*[,†] Navaneetha K. Subbaiyan,[§] Francis D'Souza,*[,§] Paul A. Karr,[⊥] Mark R. J. Elsegood,[∥] Simon J. Teat,[¶] Toshiyuki Mori,[‡] and Katsuhiko Ariga[†]

[†]*Supermolecules Group, WPI Center for Materials Nanoarchitectonics, National Institute for Materials Science, Namiki 1-1, Tsukuba, Ibaraki 305-0044, Japan,* [‡]*Fuel Cell Materials Group, National Institute for Materials Science, Namiki 1-1, Tsukuba, Ibaraki 305-0044, Japan,* [§]*Department of Chemistry, Wichita State University, 1845 Fairmount, Wichita, Kansas 67260-0051,* [⊥]*Department of Physical Sciences and Mathematics, Carhart Science 320, Wayne State College, 1111 Main Street, Wayne, Nebraska 68787,* [∥]*Chemistry Department, Loughborough University, Loughborough, Leicestershire, United Kingdom LE11 3TU, and* [¶]*ALS, Berkeley Lab, 1 Cyclotron Road, MS2-400, Berkeley, California 94720*

jonathan.hill@nims.go.jp; francis.dsouza@wichita.edu

Received September 1, 2009

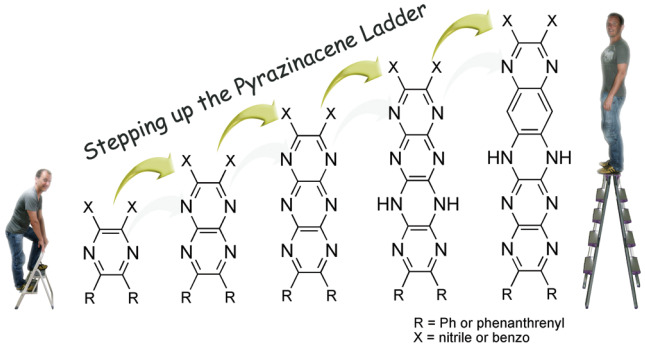

A series of edge-sharing condensed oligopyrazine analogues of acenes, the pyrazinacenes, were synthesized and characterized. X-ray crystallographic determinations revealed intermolecular interactions that affect the propensity of the molecules to undergo $\pi-\pi$ stacking. Increasing heteroatom substitution of the acene framework induces shorter intermolecular $\pi-\pi$ stacking distances (shorter than for graphite) probably due to lower van der Waals radius of nitrogen atoms. Hydrogen bonding is also a determining factor in the case of compounds containing reduced pyrazine rings. Combined electrochemical, electronic absorption, and computational investigations indicate the substantial electron deficiency of the compounds composed of fused pyrazine rings. The pyrazinacenes are expected to be good candidates as materials for organic thin film transistors.

Introduction

Acenes are aromatic compounds composed of condensed arrays of edge-sharing five- or six-membered rings, which sometimes contain heteroatoms such as sulfur or nitrogen.[1] Probably the best known of the acenes is pentacene (Scheme 1), which has attracted attention because of its solid state semiconducting properties.[2] There is currently significant interest in developing pentacene and other organic molecular semiconducting materials because of their likely application in various nascent technologies including organic field effect transistors (OFETs)[3] and photovoltaic cells.[4] While pentacene is a p-type semiconductor in the solid state, N-substituted oligoacenes are expected to be

(1) (a) Clar, E. *Polycyclic Hydrocarbons*; Academic Press: London, 1964; Vols. 1, 2. (b) Bjorseth, A., Ed. *Handbook of Polycyclic Aromatic Hydrocarbons*; Dekker: New York, 1983. (c) Harvey, R. G. *Polycyclic Aromatic Hydrocarbons*; Wiley-VCH: New York, 1997. (d) Bendikov, M.; Wudl, F.; Perepichka, D. F. *Chem. Rev.* **2004**, *104*, 4891.

(2) (a) Bailey, W. J.; Madoff, M. *J. Am. Chem. Soc.* **1953**, *20*, 5603. (b) Nickel, B.; Fiebig, M.; Schiefer, S.; Goellner, M.; Huth, M.; Erlen, C.; Lugli, P. *Phys. Status Solidi A* **2008**, *205*, 526–533. (c) Ruiz, R.; Choudhary, D.; Nickel, B.; Toccoli, T; Chang, K.-C.; Mayer, A. C.; Clancy, P.; Blakely, J. M.; Headrick, R. L.; Iannotta, S.; Malliaras, G. G. *Chem. Mater.* **2004**, *16*, 4497–4508. (d) Klauk, H.; Halik, M.; Zschieschang, U.; Schmidt, G.; Radlik, W.; Weber, W. *J. Appl. Phys.* **2002**, *92*, 5259.

Published on Web 11/02/2009 DOI: 10.1021/jo901832n

SCHEME 1. Chemical Structures of the Pyrazinacenes and Related Compounds

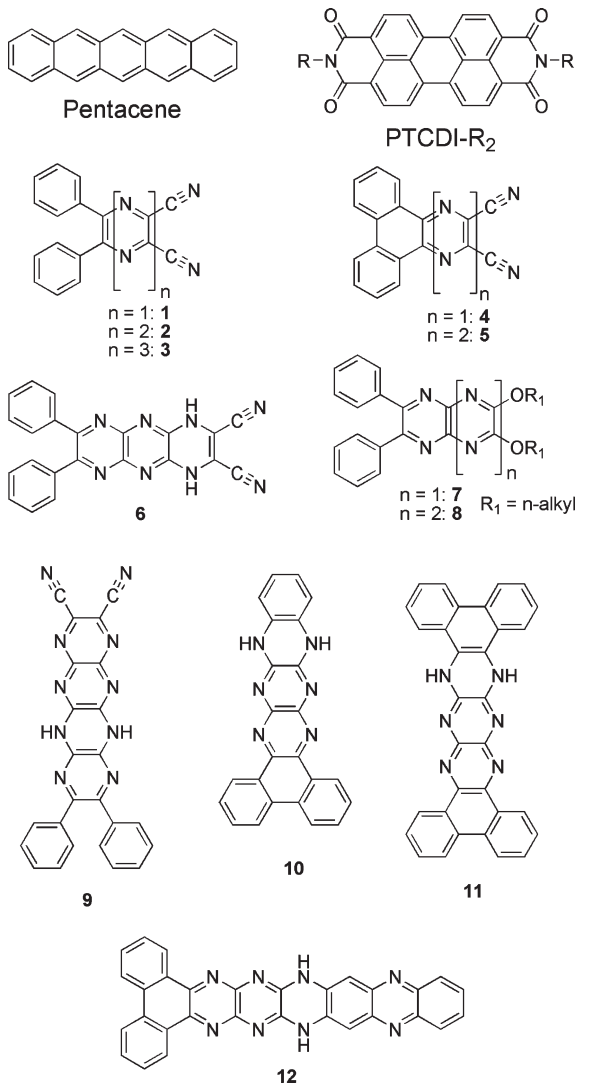

promising candidates for n-type device applications because of their high electron affinities.[5] They also have other properties of significant interest.[6] The compounds are less susceptible to degradation through oxidation or dimerization than their non-aza-substituted cousins due to their predicted electron deficiencies, although preparation of compounds having multiple edge-sharing pyrazine groups usually involves several synthetic steps.

Despite the promise of the N-substituted oligoacenes in various applications, there are only a few reports regarding their synthesis and properties. Fluorubine,[7] octaazadihydrohexacenes,[8] and decaazapentacenes[9] have been synthesized, but their semiconducting properties were not investigated, usually because of inappropriate elaboration at the molecules' periphery. Stöckner and co-workers synthesized a series of oligoazaacene-type compounds, and those molecules present excellent opportunities for studying the properties of chromophores formed from extended azaacenes.[10] Other workers have also prepared aza-substituted acenes apparently in anticipation of useful n-type semiconducting properties.[11]

Recently, computational methods based on density functional theory (DFT) have been used to highlight the potential importance of the acene family of compounds.[5,12] In particular, a diradical character of the ground state in higher oligoacenes such as heptacene was predicted by Bendikov et al.[12a] For aza-substituted acenes, it was suggested that incorporation of only five nitrogen atoms (into pentacene) is required to obtain properties of the molecules suitable for their use as n-type organic semiconducting materials.[13] Incidentally, introduction of nitrile groups at the periphery of oligoazapentacenes was found computationally to improve electron affinities and reorganizational energies, which are important for any potential organic electronic applications.

(3) (a) Horowitz, G. *Adv. Mater.* **1998**, *10*, 365–377. (b) Halik, M.; Klauk, H.; Zschieschang, U.; Kriem, T.; Schmid, G.; Radlik, W.; Wussow, K. *Appl. Phys. Lett.* **2002**, *81*, 289–291. (c) Zhang, Y.; Petta, J. R.; Ambily, S.; Shen, Y.; Ralph, D. C.; Malliaras, G. G. *Adv. Mater.* **2003**, *15*, 1632–1635. (d) Park, J. G.; Vasic, R.; Brooks, J. S.; Anthony, J. E. *J. Appl. Phys.* **2006**, *100*, 044511/1–044511/6. (e) Okamoto, T.; Senatore, M. L.; Ling, M.-M.; Mallik, A. B.; Tang, M. L.; Bao, Z. *Adv. Mater.* **2007**, *19*, 3381–3384. (f) Briseno, A. L.; Mannsfeld, S. C. B.; Ling, M. M.; Liu, S.; Tseng, R. J.; Reese, C.; Roberts, M. E.; Yang, Y.; Wudl, F.; Bao, Z. *Nature* **2006**, *444*, 913–917. (g) Newman, C. R.; Chesterfield, R. J.; Panzer, M. J.; Frisbie, C. D. *J. Appl. Phys.* **2005**, *98*, 084506/1–084506/6. (h) Kitamura, M.; Arakawa, Y. *J. Phys. (Paris)* **2008**, *20*, 184011/1–184011/16. (i) Meng, H.; Bendikov, M.; Mitchell, G.; Helgeson, R.; Wudl, F.; Bao, Z.; Siegrist, T.; Kloc, C.; Chen, C.-H. *Adv. Mater.* **2003**, *15*, 1090–1093.

(4) (a) Yoo, S.; Domercq, B.; Kippelen, B. *Appl. Phys. Lett.* **2004**, *85*, 5427–5429. (b) Pandey, A. K.; Unni, K. N. N.; Nunzi, J.-M. *Thin Solid Films* **2006**, *511−512*, 529–532. (c) Lloyd, M. T.; Mayer, A. C.; Tayi, A. S.; Bowen, A. M.; Kasen, T. G.; Herman, D. J.; Mourey, D. A.; Anthony, J. E.; Malliaras, G. G. *Org. Electron.* **2006**, *7*, 243–248. (d) Pandey, A. K.; Nunzi, J.-M. *Appl. Phys. Lett.* **2006**, *89*, 213506/1–213506/3. (e) Lim, Y.-F.; Shu, Y.; Parkin, S. R.; Anthony, J. E.; Malliaras, G. G. *J. Mater. Chem.* **2009**, *19*, 3049–3056. (f) Kim, J.-H.; Huh, S.-Y.; Kim, T.; Lee, H. H. *Appl. Phys. Lett.* **2008**, *93*, 143305/1–143305/3. (g) Palilis, L. C.; Lane, P. A.; Kushto, G. P.; Purushothaman, B.; Anthony, J. E.; Kafafi, Z. H. *Org. Electron.* **2008**, *9*, 747–752. (h) Sullivan, P.; Jones, T. S. *Org. Electron.* **2008**, *9*, 656–660. (i) Harada, K.; Riede, M.; Leo, K.; Hild, O. R.; Elliott, C. M. *Phys. Rev. B* **2008**, *77*, 195212/1–195212/9.

(5) (a) Winkler, M.; Houk, K. N. *J. Am. Chem. Soc.* **2007**, *129*, 1805–1815. (b) Constantinides, C. P.; Koutentis, P. A.; Schatz, J. *J. Am. Chem. Soc.* **2004**, *126*, 16232–16241.

(6) For example: (a) Hutchison, K.; Srdanov, G.; Hicks, R.; Yu, H.; Wudl, F. *J. Am. Chem. Soc.* **1998**, *120*, 2989–2990. (b) Langer, P.; Amiri, S.; Bodtke, A.; Saleh, N. N. R.; Weisz, K.; Görls, H.; Schreiner, P. R. *J. Org. Chem.* **2008**, *73*, 5048–5063. (c) Wudl, F.; Koutentis, P. A.; Weitz, A.; Ma, B.; Strassner, T.; Houk, K. N.; Khan, S. I. *Pure Appl. Chem.* **1999**, *71*, 295–302.

(7) (a) Akimoto, Y. *Bull. Chem. Soc. Jpn.* **1956**, *29*, 460–464. (b) Riedel, G.; Deuschel, W. UK Patent GB 970472 19640923, **1964**.

(8) Kawai, S.; Ikegami, A. *Nippon Kagaku* **1959**, *80*, 555–556.

(9) Saso, H.; Takahashi, T. JP Patent 2004189674 A2 20040708, Jpn. Kokai Tokkyo Koho, **2004**.

(10) (a) Stöckner, F.; Beckert, R.; Gleich, D.; Birckner, E.; Günther, W.; Görls, H.; Vaughan, G. *Eur. J. Org. Chem.* **2007**, 1237–1243. (b) Beckert, R.; Stöckner, F. German Patent DE 102006031752 A1 20080110, **2008**.

(11) (a) Nishida, J.; Naraso; Murai, S.; Fujiwara, E.; Tada, H.; Tomura, M.; Yamashita, Y. *Org. Lett.* **2004**, *6*, 2007–2010. (b) Nakagawa, T.; Kumaki, D.; Nishida, J.; Tokito, S.; Yamashita, Y. *Chem. Mater.* **2008**, *20*, 2615–2617. (c) Nishida, J.; Murakami, S.; Tada, H.; Yamashita, Y. *Chem. Lett.* **2006**, *35*, 1236–1237. (d) Kojima, T.; Nishida, J.; Tokito, S.; Tada, H.; Yamashita, Y. *Chem. Commun.* **2007**, 1430–1432. (e) Lee, D.-C.; Jang, K.; McGrath, K. K.; Uy, R.; Robins, K. A.; Hatchett, D. W. *Chem. Mater.* **2008**, *20*, 3688–3695. (f) Lee, D.-C.; McGrath, K. K.; Jang, K. *Chem. Commun.* **2008**, 3636–3638. (g) Lucas, L. A.; DeLongchamp, D. M.; Richter, L. J.; Kline, R. J.; Fischer, D. A.; Kaafarani, B. R.; Jabbour, G. E. *Chem. Mater.* **2008**, *20*, 5743–5749. (h) Hu, J.; Zhang, D.; Jin, S.; Cheng, S. Z. D.; Harris, F. W. *Chem. Mater.* **2004**, *16*, 4912–4915. (i) Kaafarani, B. R.; Lucas, L. A.; Wex, B.; Jabbour, G. E. *Tetrahedron Lett.* **2007**, *48*, 5995–5998. (j) Gao, B.; Wang, M.; Cheng, Y.; Wang, L.; Jing, X.; Wang, F. *J. Am. Chem. Soc.* **2008**, *130*, 8297–8306.

(12) (a) Bendikov, M.; Duong, H. M.; Starkey, K.; Houk, K. N.; Carter, E. A.; Wudl, F. *J. Am. Chem. Soc.* **2004**, *126*, 7416–7417. (b) Kenneth, B.; Wiberg *J. Org. Chem.* **1997**, *62*, 5720–5727. (c) Phukan, A. K.; Kalagi, R. P.; Gadre, S. R.; Jemmis, E. D. *Inorg. Chem.* **2004**, *43*, 5824.

(13) Chen, H.-Y.; Chao, I. *Chem. Phys. Chem.* **2006**, *7*, 2003–2007.

Here we present a method for the synthesis, several X-ray structures, and some properties of acenes composed of fused pyrazines/dihydropyrazines, compounds which we refer to as the pyrazinacenes. We investigated the electrochemical properties of the compounds and assessed their electronic structures using standard computational methods. The procedures employed in the synthesis of these compounds will permit some flexibility in the introduction of functionality as peripheral groups or by attachment at the aza-substituted molecular core.[14]

Synthesis

Our approach to the synthesis of pyrazinacenes involves a double nucleophilic attack at the 2,3 positions of 2,3-dicyanopyrazino[2,3-*b*]pyrazine derivatives, which ultimately results in substitution of both nitrile groups during the formation of an *N*,*N*′-dihydropyrazine ring. We developed this synthesis in the knowledge that TCNQ undergoes a similar double nucleophilic substitution of two of its nitrile groups by amines or alcohols.[15,16] This reaction has been investigated by several groups for preparation of self-assembling or nonlinear optically active derivatives.[17,18] Attempts to prepare phthalocyanines from 1,4,5,8-tetraaza-2,3-naphthalonitrile result only in substitution of its nitrile groups by an available nucleophile such as an alcohol to give aromatic ethers,[14a] as illustrated by compounds **7** and **8** in Scheme 1, or by amines such as *o*-phenylenediamines or diaminomaleonitrile to give dihydropyrazinacenes as exemplified by compounds **5** and **8**−**11** (Scheme 1). We realized that this reaction (Scheme 2) presents a useful method for preparation of discrete oligoacenes, especially fused oligopyrazines, and should also be available for application in the synthesis of other heteroatom-substituted acenes, even including substituted 8,8′-dicyanoquinodimethane derivatives.

In fact, the reaction (Scheme 2) can be used to prepare a variety of derivatives. Most dihydropyrazines are readily oxidized to the corresponding pyrazines either by sublimation under an oxygen atmosphere or simply by standing in air.[19] In contrast, the compounds presented in this work were found to be resistant to a variety of oxidants including 2,4-dichloro-5,6-dicyanobenzoquinone (DDQ), hydrogen peroxide, pyridinium chlorochromate, and Fremy's salt. Only compound **5** could be oxidized to the hexaazaanthracene, **3**, using ruthenium tetroxide prepared in situ from ruthenium(IV) oxide and sodium periodate. The stability of the compounds against oxidation is expected to be a result of the four ethenamine conjugatons involving the N lone pairs of the dihydropyrazine moieties together with extra resonance stability caused by an increase in the number of Clar rings. These effects more than offset the destabilization caused by the formally antiaromatic dihydropyrazine groups according to calculations by Wu and co-workers.[20a] Stability is also likely to be increased by delocalization of the antiaromaticity as suggested by nucleus independent chemical shift (NICS) calculations on related compounds.[20] Dicyanodihydropyrazinacene compounds **5** and **8** do not undergo further nucleophilic substitution of nitrile groups under the conditions used here. However, the oxidized compound **3** was found to react readily with alcohols, even in the absence of base at room temperature and could also be reacted with *o*-phenylenediamines to give dihydropyrazinacenes in a similar way to compounds **2** and **4**. This reactivity suggests the intriguing possibility of synthesizing extended ladder-type pyrazinacenes using a repeated stepwise nucleophilic substitution followed by oxidation. However, thus far, we have only been able to carry out a single cycle of this "step-ladder" approach to extended pyrazinacenes as oxidation of the larger dihydropyrazinacenes has not yet been achieved. Despite this, we were able to obtain extended pyrazinacenes by employing fused polycyclic aromatic diamines. Generally, the compounds possess good stabilities in air over long periods. Their stabilities probably arise from greater electron deficiencies relative to pentacene, which is known to be susceptible to oxidation under aerobic conditions.[21]

SCHEME 2. Typical Synthesis of Pyrazinacenes[a]

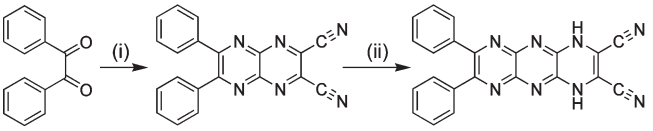

[a]Conditions: (i) 5,6-diamino-2,3-dicyanopyrazine, acetic acid/tetrahydrofuran, reflux 4 days; (ii) diaminomaleonitrile, Na_2CO_3, DMSO, 100 °C.

Results and Discussion

X-ray Crystal Structures (2, 3, 5,[14a] 8, 9). The X-ray crystal structures of several of the compounds were measured (Figure 1) and used to assess trends in the packing of the molecules in the solid state. Compounds **2**, **3**, **5**, **8**, and **9** are similarly substituted at the "ends", except that for **5** phenyl substituents are ring closed forming a diazatriphenylene unit, and **8** where nitrile groups are replaced by methoxy groups. Packing of **2** (see Supporting Information) is governed by hydrogen bonding between nitrile groups or pyrazine N atoms and CH groups of the phenyl rings. For **3** (see Figure 2), molecules are arranged so that the planes of fused pyrazine rings are all orthogonal and no stacking interactions are observed.

(14) (a) Richards, G. J.; Hill, J. P.; Okamoto, K.; Shundo, A.; Akada, M.; Elsegood, M. R. J.; Mori, T.; Ariga, K. *Langmuir* **2009**, *25*, 8408–8413. (b) Riley, A. E.; Mitchell, G. W.; Koutentis, P. A.; Bendikov, M.; Kaszynki, P.; Wudl, F.; Tolbert, S. H. *Adv. Funct. Mater.* **2003**, *13*, 531–540.

(15) Melby, L. R.; Harder, R. J.; Hertler, W. R.; Mahler, W.; Benson, R. E.; Mochel, W. E. *J. Am. Chem. Soc.* **1962**, *84*, 3374–3387.

(16) El Seoud, O. A.; Ribeiro, F. P.; Martins, A.; Brotero, P. P. *J. Org. Chem.* **1985**, *50*, 5099–5102.

(17) (a) Ravi, M.; Narayana, D. R.; Cohen, S.; Agranat, I.; Radhakrishnan, T. P. *J. Mater. Chem.* **1996**, *6*, 1119–1122. (b) Gangopadhyay, P; Sharma, S.; Rao, A. J.; Rao, D. N.; Cohen, S.; Agranat, I.; Radhakrishnan, T. P. *Chem. Mater.* **1999**, *11*, 466–472. (c) Patra, A.; Radhakrishnan, T. P. *Chem.—Eur. J.* **2009**, *15*, 2792–2800. (d) Rajesh, K.; Radhakrishnan, T. P. *Chem.—Eur. J.* **2009**, *15*, 2801–2809.

(18) (a) Li, D.; Ratner, M. A.; Marks, T. J. *J. Am. Chem. Soc.* **1988**, *110*, 1707–1715. (b) Lalama, S. J.; Singer, K. D.; Garito, A. F.; Desai, K. N. *Appl. Phys. Lett.* **1981**, *39*, 940–942.

(19) (a) Bidman, T. *Russ. J. Gen. Chem.* **2004**, *74*, 1433–1434. (b) Armand, J.; Armand, Y.; Boulares, L.; Bellec, C.; Pinson, J. *J. Heterocycl. Chem.* **1985**, *22*, 1519–1525.

(20) (a) Wu, J. I.; Wannere, C. S.; Mo, Y.; Schleyer, P. v. R.; Bunz, U. H. F. *J. Org. Chem.* **2009**, *74*, 4343–4349. (b) Miao, S.; Brombosz, S. M.; Schleyer, P. v. R.; Wu, J. I.; Barlow, S.; Marder, S. R.; Hardcastle, K. I.; Bunz, U. H. F. *J. Am. Chem. Soc.* **2008**, *130*, 7339–7344.

(21) De Angelis, F.; Gaspari, M.; Procopio, A.; Cuda, G.; Di Fabrizio, E. *Chem. Phys. Lett.* **2009**, *468*, 193–196. and references cited therein.

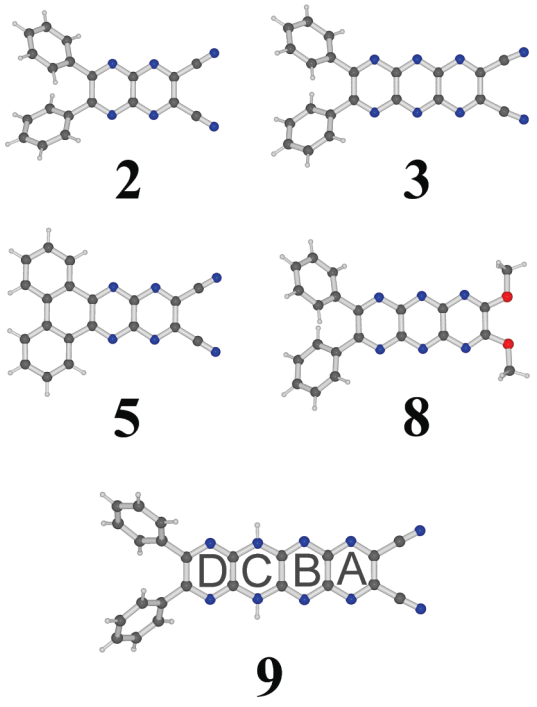

FIGURE 1. X-ray crystallographic molecular structures of **2**, **3**, **5**,[14a] **8**, and **9**.

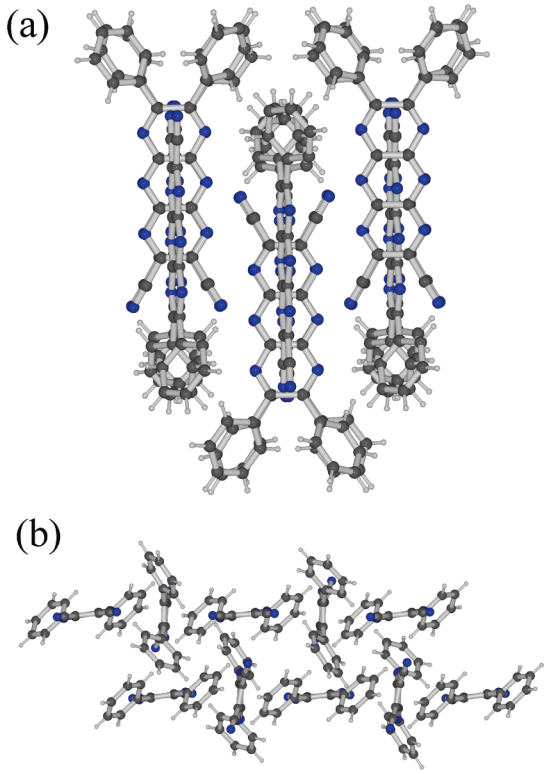

FIGURE 2. Crystal packing of **3**. (a) Viewed along *a*-axis, (b) viewed along *b*-axis. Note the orthogonal disposition of the hexaazaanthracene moieties.

There are significant close contacts between pyrazine N atoms and atoms in adjacent hexaazaanthracene moieties of neighboring molecules and a short contact between one of the nitrile groups and an adjacent C−C bond (see Figure 3). These short distances are consistent with the smaller van der Waals radius of nitrogen, which leads to a minimum contact distance between N and C of around ~3.20 Å. Although in the case of **3** there is an edge-to-face arrangement of pyrazinacene moieties, we note that the introduction of more nitrogen atoms into the acene framework should result in closer average intermolecular distances even in $\pi-\pi$ stacked structures. If nitrile groups are replaced with a non-H-bonding group such as OCH_3 as in **8**, then a $\pi-\pi$ stacked structure is obtained (Figure 3) with molecules arranged in an antiparallel fashion. The nitrile groups' H-bonding with phenyl methine groups appears to preclude formation of a stacked structure in **3** (and **2**). Conversely, if the phenyl groups are forced planar by formation of the triphenylene unit (as in **5**; see ref 14a), then all nitriles and methane groups are coplanar and a stacked structure was obtained. The shortest intermolecular distance in **8** is 3.1975(20) Å, close to the ideal length for a C−N van der Waals contact.

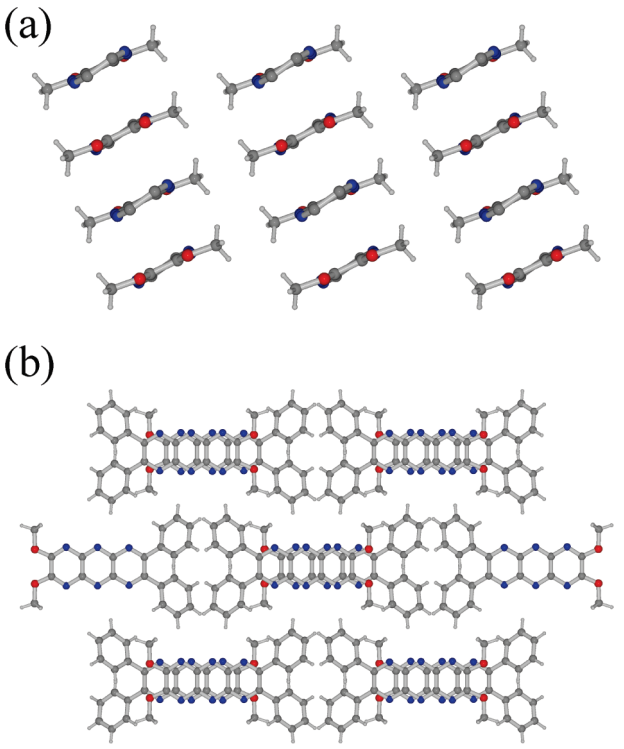

FIGURE 3. Crystal packing of **8**. (a) Viewed along *b*-axis, (b) viewed along *c*-axis. Molecules have an alternating stacked arrangement.

In the case of **9**, an apparent additional H-bonding between nitriles and dihydropyrazine units in adjacent molecules results in a partially overlapped motif (Figure 4) (again with an antiparallel arrangement of adjacent molecules in a single stack). This is significant in that it indicates a further possible way for influencing the solid state structure (and hence the properties) of these molecules. C−H−π interactions are absent in the pyrazinacene portion of the molecules, although such interactions mediate interstack organization. Nitrile groups of **9** do not interact with phenyl CHs most likely because of the greater acidity of the dihydropyrazine protons. Finally, crystals of **9** contain two molecules of tetrahydrofuran per molecule, which are also

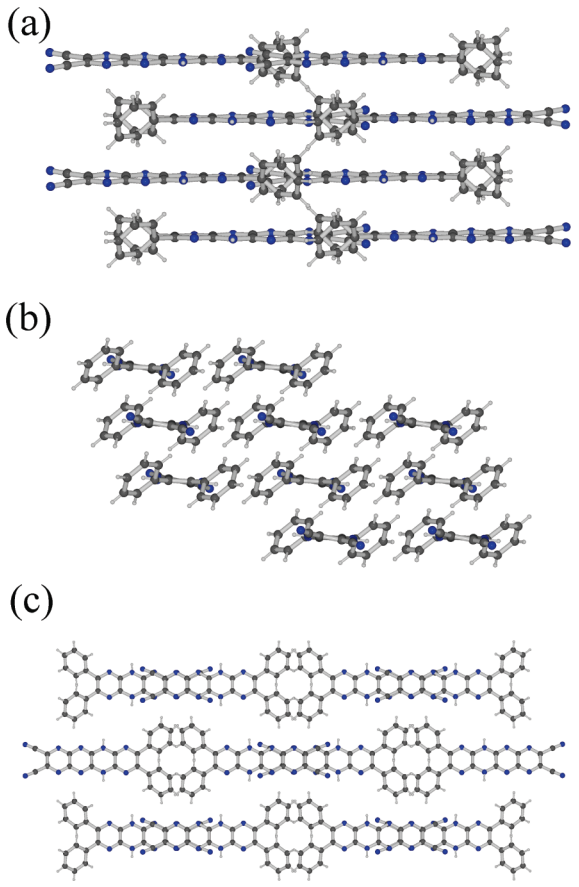

FIGURE 4. Crystal packing of **9**. (a) Viewed along *a*-axis, (b) viewed along *b*-axis, (c) viewed along *c*-axis. Antiparallel stacking is governed by hydrogen bonding. Two tetrahydrofuran molecules per **9** (H-bonded at NH groups) are omitted for clarity.

hydrogen bonded at the dihydropyrazine unit. All of the diphenyl-substituted pyrazinacenes are twisted from planarity, although this can be mostly attributed to the steric hindrance of the two phenyl groups since this effect is absent from the diazatriphenylene-type derivatives **4** and **5**. Unfortunately, the higher pyrazinacenes **10**−**12** are relatively intractable and could not be crystallized in a form suitable for single-crystal X-ray analysis, although these compounds can form other structures when appropriately substituted.[14a]

Perhaps the most intriguing finding of our single-crystal X-ray analyses comes from the location of the protons in compound **9**. The condensation of **2** with 5,6-diamino-2,3-dicyanopyrazine should yield a compound reduced at the adjacent six-membered ring (i.e., ring B rather than ring C, Scheme 1). Thus, tautomerization has occurred from the expected product giving **9**. Currently, it is unclear at which point during the preparation and isolation of **9** does this change occur, although the compound undergoes solvatochromism which might be related to tautomerism. Additionally, crystallizations of **9** occasionally yielded mixtures of differently colored crystals, although this could be due to oxidative processes since crystals of **3** were actually obtained during attempts to crystallize **6**. It is currently unclear at which point during crystallization does oxidation to **3** occur. Tautomerization in reduced polyazaacenes[22] has been investigated previously, and these compounds have attracted attention as models for the study of aromaticity and molecular orbital theory.[5,12,13,20]

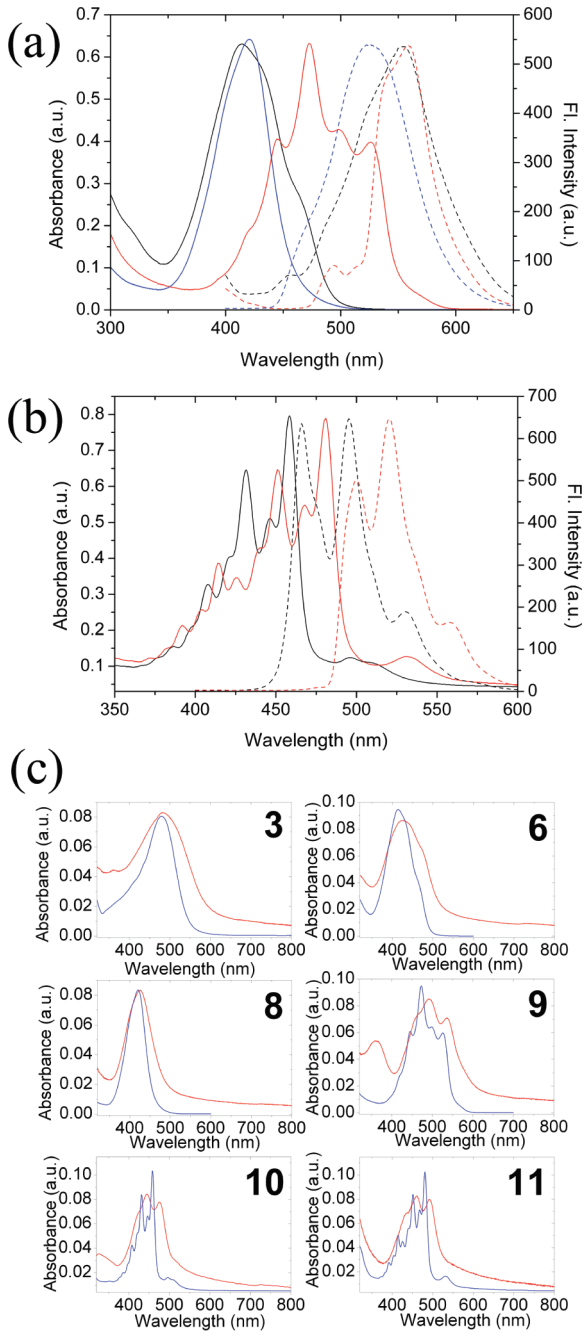

FIGURE 5. Electronic absorption spectra (solid lines) and fluorescence spectra (dashed line) of selected compounds in benzonitrile: (a) **6** (black), **8** (blue), and **9** (red); (b) **10** (black) and **11** (red). (c) Comparison of the solution state spectra (blue line) and solid state spectra (red line) of compounds **3**, **6**, **8**, **9**, **10**, and **11**.

Optical Absorption Studies. As shown in Figure 5, there is a systematic red shift in their electronic absorption maxima with increasing multiplicity of fused rings, as expected. Comparing the fused ring compound **5** with the nonfused ring analogue, **2**, a 20 nm red shift of the absorption maxima

(22) (a) Sawtschenko, L.; Jobst, K.; Neudeck, A.; Dunsch, L. *Electrochim. Acta* **1996**, *41*, 123–131. (b) Tang, Q.; Liu, J.; Chan, H. S.; Miao, Q. *Chem.—Eur. J.* **2009**, *15*, 3965–3969.

is observed for the fused ring compound. This is expected, as the phenyl rings of compound **2** are twisted relative to the plane of the molecule preventing efficient π-electronic overlap and causing a reduction in overall effective conjugation length. A comparison of the dibenzo compound **10** with the tetrabenzo compound **11** reveals a 23 nm red shift in the absorption maximum in the case of compound **11**, again, most likely due to an increase in overall conjugation length. This observation also suggests that the antiaromatic dihydropyrazine rings do not separate the molecules into two electronically discrete moieties as a simple resonance structure analysis might suggest. Fine structure emerges in the electronic absorption spectra and fluorescence spectra of compounds containing a greater number of fused rings, and this can be associated with acene-like electronic structure again despite the presence of the dihydropyrazine ring.

The electronic absorption spectra of **3**, **6**, **8**, **9**, **10**, and **11** in the thin film state (red lines) are also shown in Figure 3c in comparison with their solution state spectra (blue lines). For the compounds containing fewer fused rings, there is little difference except for some broadening, which is expected when measuring from thin solid films. This probably reflects a lack of any specific aggregation of the compounds in the solution or solid states. **9** is notable in that it possesses an extra band at shorter wavelength around 360 nm when measured in the solid state. Such bands are often observed in compounds that tend to aggregate as stacks (so-called H-aggregation), and this is partly consistent with its X-ray crystal structure. In solution, both **10** and **11** possess weak bands at 500 and 540 nm, respectively, also suggesting aggregation. In the solid state, the UV/vis spectra of **10** and **11** are broadened and undergo a relative increase in absorbance of bands at shorter wavelength, although no additional absorption bands appear. Acene aggregation has been studied by Desvergne and co-workers,[23] and they also observed a lower energy band in substituted tetracene derivatives assigning it to a $\pi-\pi$ stacking mode. In **10** and **11**, similar bands can be observed, but these are present also in the solution state. The study of gelated states of suitably substituted derivatives will lead to a better understanding of these aggregation processes, which are critical for electronic coupling in organic chromophoric compounds.

Electrochemistry. Cyclic voltammetric (CV) data of compounds **2**−**6** and **8**−**12** are summarized in Table 1. Soluble compounds were studied in dry benzonitrile, while the higher pyrazinacenes could only be dissolved in tetrahydrofuran or dimethylsulfoxide for CV investigations. Compounds without reduced rings gave well-defined reduction waves, while the redox behaviors of those bearing a dihydropyrazine ring are more complex. Cyclic voltammograms are shown in Figure 6.

In the compounds containing fewer pyrazine rings, it is possible to observe the effect of some of the structural variations. Thus, the difference between compounds **2** and **5** is an oxidative ring closure at the phenyl rings of **2** giving **5**, which leads to a cathodic shift of the reduction waves (0.13 and 0.23 V for the first and second reductions, respectively). Also, a much more significant cathodic shift of the reduction waves is observed by increasing the number of condensed pyrazine rings passing from **2** to **3** (0.52 and 0.72 V for the first and second reductions, respectively). Conversely, replacing nitrile groups in **3** with methoxy groups (**8**) results in an anodic shift of −0.96 and −0.71 V for the first and second reductions, respectively, although compound **8** remains stable against oxidization over the voltage range studied. **6** can be considered a reduced form of **3** with the former being electron-rich compared to **3**. Thus, an oxidation wave is observed, and **6** requires a more negative potential for reduction. Compound **9** has redox behavior similar to that of **6**, although the additional pyrazine ring has the now predictable effect of cathodically shifting its first reduction potential. Compounds **10**−**12** show some evidence for being susceptible to oxidation as expected from the presence of the dihydropyrazine group, but redox waves are poorly defined. Measurement of these compounds is complicated by the requirement of a polar solvent for the analysis so that proton-coupled reactions including tautomerism and deprotonation are more likely to occur under such conditions.

TABLE 1. Electrochemical Properties of Compounds 2−6 and 8−11 in Benzonitrile Containing 0.1 M n-Bu_4NClO_4 at a Scan Rate of 100 mV/s

compound	first ox[a]	first red[a]	second red[a]
2	−	−0.76	−1.63
3	−	−0.24	−0.91
4	−	−1.51[b]	−
5	−	−0.63[c]	−1.40[c]
6	0.47	−1.43	−
8	−	−1.2	−1.62
9	0.32	−1.17	−1.72
10	0.20	−1.78	−
11	0.69	−1.92	−

[a]Oxidation and reduction potentials vs ferrocene. [b]See ref 11a. [c]This work. Compared to −0.70 (first red) and −1.48 (second red)[11a].

From these data, we surmise that both oxidative ring closure and increased pyrazine multiplicity favor electron deficiency while compounds containing dihydropyrazine or alkoxy groups are relatively electron-rich. In semiconductor material parlance then perhaps we have access to both n- and p-type molecules within the same compound class. On a related subject, [6,6]-phenyl-C_{61} butyric acid methyl ester (PCBM) is a fullerene C_{60}-based compound commonly used as an electron-accepting material in organic photovoltaic (OPV) devices. PCBM has a LUMO of −3.75 eV and a HOMO of −5.8 eV as determined by cyclic voltammetry.[24] With the exception of compounds **10**−**12**, the compounds presented in this work show LUMO levels comparable with PCBM, perhaps suggesting that these compounds or, for example, polymeric derivatives might find application as electron-accepting materials in OPVs.

Computational Analysis. 2−**6** and **8**−**12** were modeled using DFT[25] at the B3LYP/6-31G(d,p) level in order to predict the relative HOMO and LUMO energy levels. The levels could also be determined to some extent experimentally using cyclic voltammetry and UV/vis absorption spectroscopy. The relevant data obtained from those analyses are contained in Table 2.

HOMO and LUMO levels are stabilized with an increase in the number of pyrazine units and destabilized in the reduced *N*,*N*-dihydropyrazine forms. This can be rationalized in terms of the overall electron deficiency of the

(23) (a) Desvergne, J.-P.; Brotin, T.; Meerschaut, D.; Clavier, G.; Placin, F.; Pozzo, J.-L.; Bouas-Laurent, H. *New J. Chem.* **2004**, *28*, 234. (b) Desvergne, J.-P.; Del Guerzo, A.; Bouas-Laurent, H.; Belin, C.; Reichwagen, J.; Hopf, H. *Pure Appl. Chem.* **2006**, *78*, 707–719.

(24) Sensfuss, S.; Al-Ibrahim, M. In *Organic Photovoltaics*, Sun, S., Sariciftci, N. S., Eds.; CRC Press: Boca Raton, FL, 2004; Vol. 23, p 529.

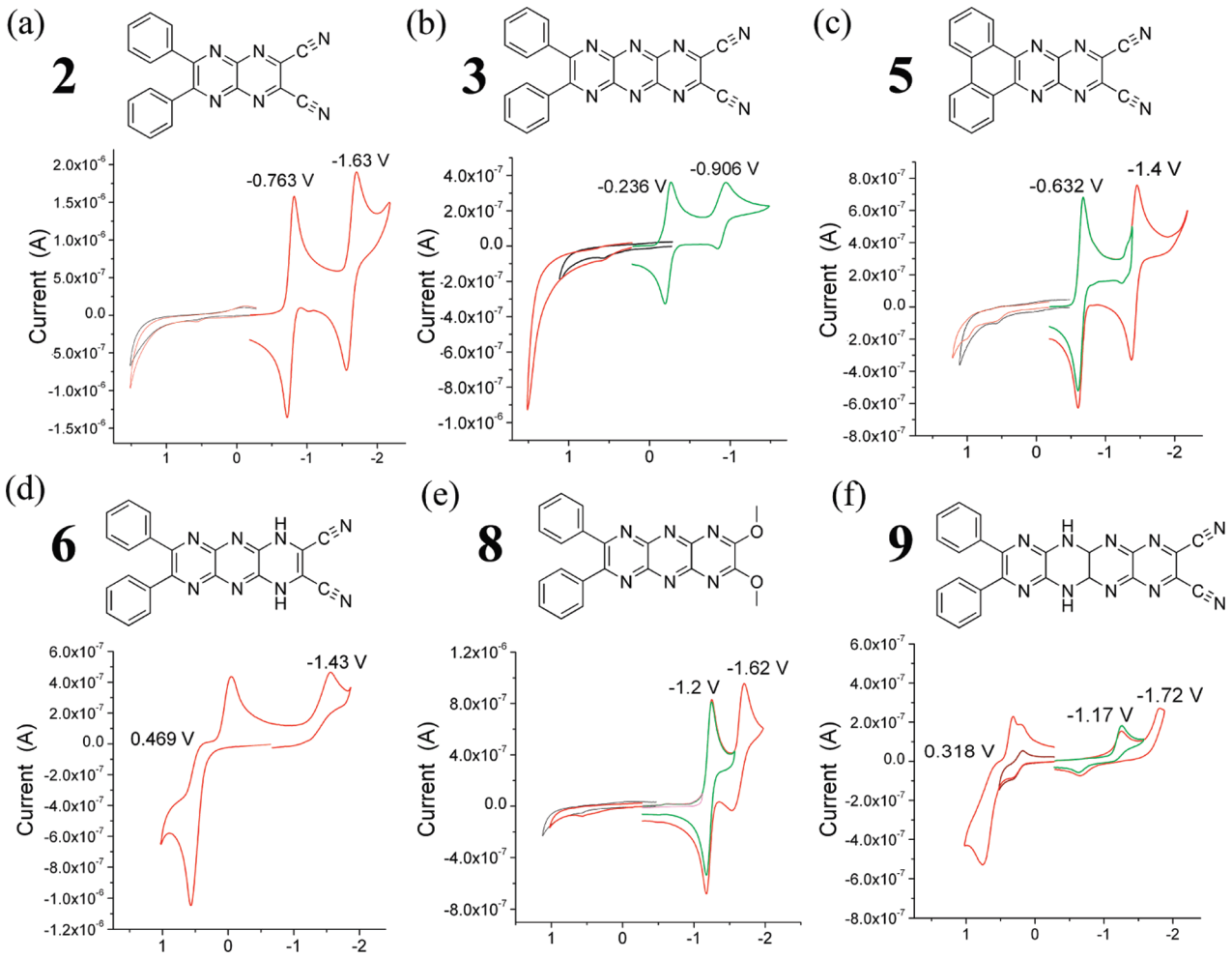

FIGURE 6. Electrochemical behaviors of **2**, **3**, **5**,[11a] **6**, **8**, and **9** in benzonitrile containing 0.1 M *n*-Bu_4NClO_4 at a scan rate 100 mV/s.

system—more pyrazine groups will tend to increase electron deficiency, causing a stabilization of the HOMO and LUMO, whereas reduced pyrazines are more electron-rich, so a destabilization of the HOMO/LUMO levels is expected. A similar pattern can be observed when comparing the dicyano- and dimethoxy-hexaazaanthracene compounds **3** and **8**, respectively. Due to the electron-deficient nature of the pyrazine ring system, all of the compounds have low-lying HOMOs—even in the case of the reduced pyrazine compounds. This may account for the high stability of the compounds toward oxidation. Although the phenazine compounds tend to have comparatively destabilized HOMOs, due to the higher ratio of more electron-rich phenyl rings, we could not oxidize these compounds using similar conditions to those used to oxidize **6**, although their very low solubility in mixtures of carbon tetrachloride and acetonitrile necessary for the oxidation reaction complicated matters.[26] The dicyano-tetraazanapthalene compounds **2** and **5** have low-lying HOMO and LUMO levels, which partly accounts for their unusual reactivity toward nucleophiles. The dicyano-hexaazaanthracene compound **3** has even lower-lying frontier orbitals, suggesting even greater reactivity toward nucleophilic substitution, accounting for the high reactivity of this compound even toward aliphatic alcohols at room temperature. Modeling of higher pyrazinacenes in their oxidized form suggests even higher electron affinities and ionization potentials, and it is likely that similar reactivity will be observed for those compounds.

As mentioned previously, **2**, **3**, **5**, and **8** exhibit two fully or quasi-reversible reduction peaks, and with the exception of compound **12**, all of the other compounds exhibit irreversible first reduction peaks. The first reduction peaks were used to estimate the LUMO energy level of the molecules, and the frontier energy levels were also estimated using DFT methods. The optical band gaps of the molecules were determined from their UV/vis absorption spectra in dilute solution. The

(25) Frisch, M. J.; Trucks, G. W.; Schlegel, H. B.; Scuseria, G. E.; Robb, M. A.; Cheeseman, J. R.; Montgomery, J. A.; Vreven, T.; Kudin, K. N.; Burant, J. C.; Millam, J. M.; Iyengar, S. S.; Tomasi, J.; Barone, V.; Mennucci, B.; Cossi, M.; Scalmani, G.; Rega, N.; Petersson, G. A.; Nakatsuji, H.; Hada, M.; Ehara, M.; Toyota, K.; Fukuda, R.; Hasegawa, J.; Ishida, M.; Nakajima, T.; Honda, Y.; Kitao, O.; Nakai, H.; Klene, M.; Li, X.; Knox, J. E.; Hratchian, H. P.; Cross, J. B.; Bakken, V.; Adamo, C.; Jaramillo, J.; Gomperts, R.; Stratmann, R. E.; Yazyev, O.; Austin, A. J.; Cammi, R.; Pomelli, C.; Ochterski, J. W.; Ayala, P. Y.; Morokuma, K.; Voth, G. A.; Salvador, P.; Dannenberg, J. J.; Zakrzewski, V. G.; Dapprich, S.; Daniels, A. D.; Strain, M. C.; Farkas, O.; Malick, D. K.; Rabuck, A. D.; Raghavachari, K.; Foresman, J. B.; Ortiz, J. V.; Cui, Q.; Baboul, A. G.; Clifford, S.; Cioslowski, J.; Stefanov, B. B.; Liu, G.; Liashenko, A.; Piskorz, P.; Komaromi, I.; Martin, R. L.; Fox, D. J.; Keith, T.; Al-Laham, M. A.; Peng, C. Y.; Nanayakkara, A.; Challacombe, M.; Gill, P. M. W.; Johnson, B.; Chen, W.; Wong, M. W.; Gonzalez, C.; Pople, J. A. *Gaussian 03*, revision C.02; Gaussian, Inc.: Wallingford, CT, 2004.

(26) Zibuck, R; Seebach, D. *Helv. Chim. Acta* **1988**, *71*, 237–240.

TABLE 2. Energy Levels and Band Gaps of the Compounds Derived from Experimental and Computational Data

compound	E_{red}^{onset}	E_{LUMO}^{CV}	E_{LUMO}^{DFT}	$E_{HOMO}^{CV/OPT}$	E_{HOMO}^{DFT}	E_{GAP}^{OPT}	E_{GAP}^{DFT}
2	−0.69	−4.12	−3.6	−6.75	−6.88	2.63	3.28
3	−0.15	−4.65	−4.16	−6.93	−6.97	2.28	2.81
5	−0.56	−4.24	−3.76	−6.92	−6.82	2.68	3.06
6	−1.26	−3.54	−2.8	−6.22	−5.75	2.68	2.95
8	−1.14	−3.67	−2.86	−6.37	−6.09	2.7	3.23
9	−1.12	−3.68	−3.13	−5.38	−5.74	2.25	2.61
10	−1.72	−3.08	−2.05	−5.71	−5.14	2.63	3.09
11	−1.8	−3	−1.98	−5.21	−4.93	2.21	2.95
12	–	–	−2.69	–	−5.49	2.21	2.8

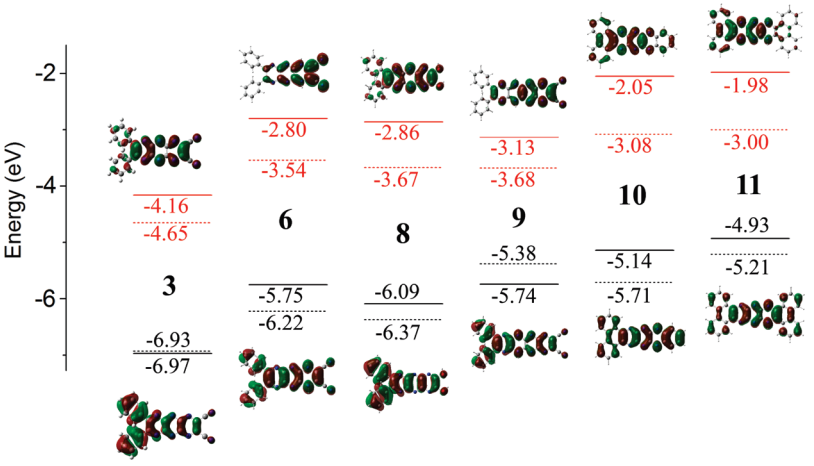

FIGURE 7. Energy levels obtained from experimental (optical/electrochemical; dashed line) and computational data (solid line), and HOMO and LUMO structures of the compounds.

HOMO energy levels were calculated by subtracting the optical band gap energy from the LUMO energy determined by cyclic voltammetry. The results are shown in Table 2. The DFT calculations overestimate the optically determined band gap by 0.50 ± 0.24 eV, and the LUMO values are overestimated by 0.71 ± 0.33 eV and the HOMO values by 0.15 ± 0.5 eV. The differences between the DFT calculations and the experimentally determined values can be easily explained because (i) DFT calculations were based on a single molecule in vacuum (no attempt was made to model solvent effects or other intermolecular forces), (ii) imperfections in the DFT model, and (iii) imperfections in the techniques used to determine the experimental values (e.g., the optical absorption edge may be difficult to determine due to "tailing" etc.). Taking these factors into account, the DFT calculations predict the electrochemical properties of these compounds reasonably well, and overall trends in electrochemical behavior are predicted with good precision. Trends in the electronic properties of the compounds are illustrated in Figure 7, where energy levels of HOMOs and LUMOs are plotted for **3**, **6**, and **8**−**11** together with the calculated structures of the respective orbitals. Of these compounds, **9** stands out as having the smallest HOMO−LUMO band gap obtained from both computational and experimental data.

Finally, we note a tendency for the calculated LUMO (for **6**) or LUMO+1 (for **2**, **5**, **8**, **9**, **10**, and **11**) structures to have a symmetrical alternating structure (see Figure 8) similar to

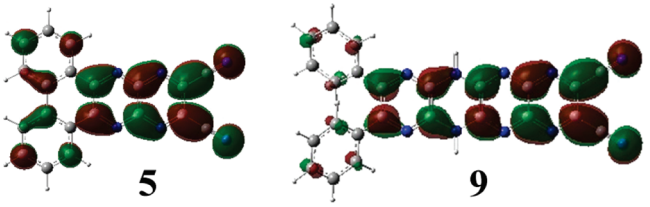

FIGURE 8. Acene-like molecular orbital structure in the LUMO+1 of **5** and **9**.

that predicted for polyacenes,[27,28] which can be seen as materials containing two weakly coupled polyacetylene chains possessing special properties,[12,29] while HOMO orbital structures of the pyrazinacenes appear to be largely due to conjugative delocalization (except for **5** where the HOMO is localized on its triphenylene unit). This implies that acene-like properties might be available in the excited states of these molecules despite the presence of a dihydropyrazine ring. Thus, we are currently speculating on the possibility of photolytically induced insulator−semiconductor switching of these molecules and their higher derivatives.

Protic compounds **9**, **10**, and **11** all exhibit oxidation peaks by cyclic voltammetry. For compound **9**, the onset of oxidation occurs around 0.17 V, suggesting HOMO level of around −4.97 eV and a band gap of 1.29 eV. These values are not consistent with either the DFT calculations or the

(27) (a) Kertesz, M.; Hoffmann, R. *Solid State Commun.* **1983**, *47*, 97–102. (b) Garcia-Bach, M. A.; Peñaranda, A.; Klein, D. J. *Phys. Rev. B* **1992**, *45*, 10891.

(28) Lowe, J. P.; Kafafi, S. A.; LaFemina, J. P. *J. Phys. Chem.* **1986**, *90*, 6602–6610.

(29) (a) Houk, K. N.; Lee, P. S.; Nendel, M. *J. Org. Chem.* **2001**, *66*, 5517–5521. (b) Kivelson, S.; Chapman, O. L. *Phys. Rev. B* **1983**, *28*, 7236.

optical measurements, and it is likely that, in the case of **9**, **10**, and **11**, the electrochemical oxidation peaks may be a result of deprotonation or tautomeric effects. Deprotonation of the dihydropyrazine-group-containing compounds is a significant issue for the azaacenes because of the presence of sites both for protonation and for deprotonation. Thus, these compounds should possess properties of acidity and basicity albeit complicated by underlying tautomerism phenomena such as in **9**. We determined the pK_a of **10** as 13.3 ± 0.1 for its first deprotonation (by titration with DBU in DMSO[30]), which is in the region of acidity of azoles, 4-pyridones, and similar unsaturated heterocyclic amines.[31] **10** resists further deprotonation using organic bases so that it is a simple matter to isolate the monoanion. Similarly, the pyrazinacenes resist protonation by organic acids beyond a monocationic species.

Conclusion

In summary, we have prepared a series of nitrogenous acenes, the pyrazinacenes, which have potential as n-type organic semiconductors. Our synthesis is facile and allows several points for elaboration of the compounds. Structural features include short interplanar distances and long distance stacking in their crystals. Hydrogen bonding can also be a determining factor in the case of compounds containing reduced pyrazine rings. Combined electrochemical, electronic absorption, and computational investigations indicate the substantial electron deficiency of the compounds composed of fused pyrazine rings, while those with one reduced ring might exhibit ambipolar behavior.

Overall, this work suggests structural features that are useful for design of materials with potential as organic components of photovoltaic or semiconduting devices and incorporation of these into appropriate aggregated or thin film structures will be of interest. The absolute structures and reactivities of the dihydro-substituted compounds described here are further subject to tautomerism phenomena, and that will be the subject of shortly forthcoming reports. Also, in this work, we found that compounds containing up to four unsubstituted edge-sharing pyrazine/dihydropyrazine rings are easily accessible in useful quantities while longer acenes are available but with non-aza-substituted benzene rings interrupting the pyrazinacene structure. Synthesis of the higher pyrazinacenes is currently underway in our laboratories. Finally, NH tautomerization is potentially a significant feature of these compounds, and we are currently studying this phenomenon, also in the higher pyrazinacenes, with respect to its effect on the acidity and basicity of these compounds.

Experimental Section

Synthesis. 2,3-Dicyano-7,8-diphenyl-1,4,5,6,9,10-hexaazaanthracene, 3. Ruthenium(IV) oxide (21 mg, 1.58×10^{-4} mol) and sodium periodate (725 mg, 3.39×10^{-3} mol) were added to a mixture of compound **6** (100 mg, 2.57×10^{-4} mol), carbon tetrachloride (5 cm^3), acetonitrile (5 cm^3), and water (2 cm^3). The mixture changed color immediately from yellow to brown/orange, and it was then stirred at room temperature for 1 h. Dichloromethane (10 cm^3) and water (10 cm^3) were added, and the organic layer was separated, dried over Na_2SO_4, filtered, and solvents were evaporated to give a brown-orange solid. The crude product was purified by dissolving in ethyl acetate and passing the solution through a pad of silica gel followed by further washing of the silica pad with ethyl acetate. The solvent was removed under reduced pressure to give the product as an orange-brown crystalline solid: Yield 90 mg (91%); ^{1}H NMR (300 MHz, CD_3CN, 70 °C) δ = 7.77 (m, 4H, Ar*H*), 7.58 (m, 2H, Ar*H*), 7.47 (m, 4H, Ar*H*) ppm; MALDI-TOF-MS (dithranol) calcd for $C_{22}H_{10}N_8$ m/z = 386.1, found m/z = 389.1 $[M + 3H]^+$. Compound **3** did not afford satisfactory combustion analysis.

2,3-Dicyano-1,4-dihydro-7,8-diphenyl-1,4,5,6,9,10-hexaazaanthracene, 6. A mixture of 2,3-dicyano-6,7-diphenyl-1,4,5,8-tetraazanapthalene (0.7 g, 2.10×10^{-3} mol), diaminomaleonitrile (0.5 g, 4.63×10^{-3} mol), and sodium carbonate (0.9 g, 8.50×10^{-3} mol) in dimethylsulfoxide (25 cm^3) was heated at 80 °C for 4 h. The mixture was added to water (300 cm^3) and extracted with dichloromethane (200 cm^3) followed by ethyl acetate (2×400 cm^3). The organic extracts were combined, dried over Na_2SO_4, filtered, and concentrated to a black solid. The crude product was purified by column chromatography three times (silica gel, dichloromethane eluting to 5% methanol in dichloromethane) to give the product as a yellow-orange solid after evaporation of solvent under reduced pressure: Yield 430 mg (53%); ^{1}H NMR (300 MHz, DMSO-d_6, 25 °C) δ = 11.40 (s, 2H, N*H*), 7.23 (m, 10H, Ar*H*) ppm; IR (BaF_2 disk) ν = 3170 (m), 3086 (m), 3021 (m), 2916 (m), 2851 (m), 2759 (m), 2231 (m, CN stretch), 1570 (m, C=C stretch), 1511 (s, C=N stretch), 1492 (s), 1476 (m), 1465 (m), 1445 (s, C−C stretch), 1410 (s), 1316 (m), 1194 (m); UV/vis (λ_{max}) 415 (ε = 26 100 mol^{-1} cm^{-1}) nm; LDI-TOF-MS calcd for $C_{22}H_{12}N_8$ m/z = 388.10, found m/z = 389.02 $[M + H]^+$. Anal. Calcd for $C_{22}H_{12}N_8 \cdot 1/2H_2O$: C, 66.49; H, 3.30; N, 28.20. Found: C, 66.32; H, 3.22; N, 27.81.

2,4-Dimethoxy-7,8-diphenyl-1,4,5,6,9,10-hexaazaanthracene, 8. 2,3-Dicyano-7,8-diphenyl-1,4,5,6,9,10-hexaazaanthracene (50 mg, 1.30×10^{-4} mol) was dissolved in methanol (5 cm^3), and the solution was allowed to stand at room temperature for 2 h. The solvent was removed under reduced pressure, and the residue was purified by column chromatography (neutral alumina, 5% methanol in dichloromethane) to give the product as an orange, crystalline solid: Yield 35 mg (68%); ^{1}H NMR (300 MHz, $CDCl_3$, 22 °C) δ = 7.72 (m, 4H, Ar*H*), 7.40 (m, 6H, Ar*H*), 4.38 (s, 8H, Ar*H*) ppm; IR (KBr pellet) ν = 3049 (w), 2943 (w, C−H stretch), 1621 (w), 1569 (s, C=N stretch), 1515 (m), 1463 (s), 1399 (s), 1384 (s), 1324 (m), 1266 (m), 1190 (m), 1020 (m), 723 (w, C−H bend), 700 (m), 688 (m), 597 (m) cm^{-1}; UV/vis (λ_{max}) 416 (ε = 43 600 mol^{-1} cm^{-1}) nm; MALDI-TOF-MS (dithranol) calcd for $C_{22}H_{16}N_6O_2$ m/z = 396.13, found m/z = 397.07 $[M + H]^+$. Anal. Calcd for $C_{22}H_{16}N_6O_2$: C, 66.67; H, 4.04; N, 21.21. Found: C, 66.38; H, 4.28; N, 20.86.

2,4-Dicyano-5,12-dihydro-8,9-diphenyl-1,4,5,6,7,10,11,12-octaazatetracene, 9. A mixture of 2,3-dicyano-6,7-diphenyl-1,4,5,8-tetraazanapthalene (200 mg 6.37×10^{-4} mol), 2,3-dicyano-5,6-diaminopyrazine (204 mg, 1.28×10^{-3} mol), and sodium carbonate (230 mg, 2.17×10^{-3} mol) in dimethysulfoxide (14 cm^3) was heated at 90 °C for 2 h. Ammonium chloride (200 mg) and acetic acid (200 mg) were added, and the solvent was removed under reduced pressure. The residue was dissolved in tetrahydrofuran and passed through a pad of silica gel. The solvent was removed under reduced pressure, and the residue was purified by column chromatography (silica gel, tetrahydrofuran: dichloromethane 1:1) to give the product as an orange solid which was further purified by recrystallization from tetrahydrofuran/hexane: Yield 102 mg (36%); ^{1}H NMR (300 MHz, acetone-d_6, 25 °C) δ = 7.43 (m, 10H, Ar*H*) ppm; IR (KBr pellet) ν = 3414 (NH stretch), 2924 (C−H stretch), 2221 (m, C−N stretch), 1607 (m, C−C stretch), 1511 (s), 1482 (s), 1448 (s, C−C stretch), 1421 (s), 1383 (s), 1364 (s), 1206 (s), 766 (m, C−H bend),

(30) Wu, A.; Masland, J.; Swartz, R. D.; Kaminsky, W.; Mayer, J. M. *Inorg. Chem.* **2007**, *46*, 11190–11201.
(31) Bordwell, F. G. *Acc. Chem. Res.* **1988**, *21*, 456–463.

695 (s) cm^{-1}; UV/vis (λ_{max}) 509.5 (ε = 22 400 mol^{-1} cm^{-1}), 470.5 (ε = 53 100 mol^{-1} cm^{-1}), 442.5 (ε = 38 000 mol^{-1} cm^{-1}) nm; MALDI-TOF-MS (dithranol) calcd for $C_{24}H_{12}N_{10}$ m/z = 440.12, found m/z = 441.05 $[M + H]^+$. Satisfactory elemental analysis could not be obtained although X-ray crystal structure confirms molecular structure.

5,14-Dihydro-[*l*,*n*]-dibenzo-5,6,7,12,13,14-hexaazapentacene, 10. A mixture of **5** (100 mg, 3.01×10^{-4} mol), 1,2-phenylenediamine (65 mg, 6.02×10^{-4} mol), and sodium carbonate (134 mg, 1.24×10^{-3} mol) in *N,N*-dimethylformamide (7 mL) was heated at 150 °C for 2 h. The mixture was allowed to cool to room temperature overnight, and the resulting precipitate was filtered, rinsed with dichloromethane (20 mL), hot water (3 × 25 mL), and tetrahydrofuran (20 mL) to give the product as a yellow-brown solid, which was dried under reduced pressure: Yield 45 mg (39%); ^{1}H NMR (300 MHz, DMSO-d_6, 25 °C) δ = 11.51 (s, 2H, N*H*), 8.77 (m, 4H, 2 × Ar*H*), 7.71 (m, 4H, 2 × Ar*H*), 7.39 (m, 2H, Ar*H*), 7.30 (m, 2H, Ar*H*) ppm; IR (KBr pellet) ν = 3397 (w, N−H str), 3194, (w, phenanthrene C−H str), 2925 (w, 1,2-phenylene C−H str), 1592 (m, C=C str), 1547 (m, C=N str), 1495 (m), 1481 (m), 1462 (s, C−C str), 1404 (s), 1284 (m), 1229 (m, C−N str), 762 (m), 748 (s, C−H bend), 722 (s, C−H bend), 613 (m) cm^{-1}; UV/vis (λ_{max}) 458 (ε = 70 800 mol^{-1} cm^{-1}), 446.5 (ε = 42 500 mol^{-1} cm^{-1}), 431 (59 300 mol^{-1} cm^{-1}), 407.5 (ε = 29 000 mol^{-1} cm^{-1}) nm; MALDI-TOF-MS (dithranol) calcd for $C_{24}H_{14}N_6$ m/z = 386.13, found m/z = 385.97 $[M]^+$. Anal. Calcd for $C_{24}H_{14}N_6$: C, 74.60; H, 3.65; N, 21.75. Found: C, 73.93; H, 3.83; N, 21.93.

5,14-Dihydro-[*a*,*c*,*l*,*n*]-tetrabenzo-5,6,7,12,13,14-hexaazapentacene, 11. A mixture of 2,3-dicyano-[*h*,*j*]-dibenzo-1,4,5,10-tetraazaanthracene (200 mg, 6.02×10^{-4} mol), 9,10-diaminophenanthrene (83.5 mg, 4.01×10^{-4} mol), and sodium carbonate (77 mg, 7.22×10^{-4} mol) in dimethylsulfoxide (10 cm^3) was heated at 150 °C for 2 h. The mixture was allowed to cool to room temperature and left to stand for 3 days. The resulting precipitate was filtered and washed with dichloromethane (20 cm^3), hot water (50 cm^3), and methanol (10 cm^3). Residual low molecular weight impurities were removed by sublimation to give the pure product as a pale brown solid: Yield 45 mg (23%); ^{1}H NMR (300 MHz, DMSO-d_6, 100 °C) δ = 11.10 (s, 2H, N*H*), 8.83 (m, 4H, Ar*H*), 8.72 (m, 4H, Ar*H*), 7.70 (m, 8H, Ar*H*) ppm; IR (KBr pellet) ν = 3408 (NH stretch), 3062 (CH stretch), 2961 (CH stretch), 1590 (w, C=C stretch), 1506 (w), 1458 (s, C−C stretch), 1394 (s), 1283 (m), 1227 (m), 768 (w, C−H bend), 724 (w, C−H bend), 619 (w) cm^{-1}; MALDI-TOF-MS (dithranol) calcd for $C_{32}H_{18}N_6$ m/z = 486.16, found m/z = 486.02 $[M]^+$. Satisfactory elemental analysis could not be obtained.

7,16-Dihydro-[*p*,*r*]-dibenzo-5,7,8,9,14,15,16,18-octaazaheptacene, 12. A mixture of **5** (100 mg, 3.01×10^{-4} mol), 2,3-diaminophenazine (63 mg, 3.01×10^{-4} mol), and sodium carbonate (200 mg, 1.89×10^{-3} mol) in *N,N*-dimethylformamide (10 mL) was heated at 150 °C for 2 h. The mixture was allowed to cool to room temperature overnight, and the resulting precipitate was filtered, rinsed with dichloromethane (20 mL), hot water (3 × 25 mL), and tetrahydrofuran (20 mL) to give the product as a dark brown solid: Yield 44 mg (30%); ^{1}H NMR (300 MHz, TFA-d_1, 25 °C) δ = 9.07 (m, 2H, Ar*H*), 8.74 (m, 2H, Ar*H*), 8.35 (m, 2H, Ar*H*), 8.18 (m, 2H, Ar*H*), 8.15 (s, 2H, Ar*H*), 8.01 (m, 2H, Ar*H*), 7.88 (m, 2H, Ar*H*) ppm; IR (KBr pellet) ν = 3385 (w, N−H str), 3064 (w, C−C str), 2919 (w, C−C str), 1593 (m, C−C str), 1467 (s), 1463 (s), 1421 (s), 1368 (s), 1319 (m), 1219 (s, C−N str), 1133 (m, C−N str), 757 (m, C−H bend), 723 (m, C−H bend) cm^{-1}; MALDI-TOF-MS (dithranol) calcd for $C_{30}H_{16}N_8$ m/z = 488.15, found m/z = 491.30 $[M + 2H]^+$. Anal. calcd for $C_{30}H_{16}N_8 \cdot 5/4H_2O$: C, 70.51; H, 3.65; N, 21.93. Found: C, 70.40; H, 3.53; N, 22.20.

X-ray Crystallography. Structure solutions were by direct methods and refinement with SHELXTL.[32] X-ray crystallography data for **2** (crystallized by diffusion of hexane into a dichloromethane solution of **2**) were collected at 150 K using graphite-monochromated Mo Kα radiation. $C_{20}H_8N_6$, M = 334.34 g/mol, crystal size 0.53 × 0.08 × 0.02 mm^3, yellow needle, space group $P2(1)/n$, a = 9.0585(18) Å, b = 6.9906(14) Å, c = 25.138(5) Å, β = 92.14(3)°, V = 1590.7(5) $Å^3$, Z = 4, ρ_{calcd} = 1.396 mg/m^3, μ(Mo Kα) = 0.089 mm^{-1}, 12 388 reflections were measured (2θ < 54.3°) of which 3247 were unique (R_{int} 0.0308). Refinement against F^2 to $wR2$: 0.102 (all data), $R1$ (2447 reflections with $I > 2\sigma(I)$) 0.0413, 275 parameters, no restraints; all non-H atoms were anisotropic refined.

X-ray crystallography data for **3** (crystallized by diffusion of methanol into a chloroform solution of **6** (autoxidation to **3** occurred)) were collected at 150 K using silicon 111 monochromated synchrotron radiation. $C_{22}H_{10}N_8$, M = 386.37 g/mol, crystal size 0.30 × 0.15 × 0.01 mm^3, orange plate, space group $C2/c$, a = 19.1050(16) Å, b = 38.439(3) Å, c = 13.5450(11) Å, α = 90.00°, β = 132.782(2)°, γ = 90.00°, V = 7300.6(10) $Å^3$, Z = 16, ρ_{calcd} = 1.406 mg/m^3, μ = 0.091 mm^{-1}, 43 122 reflections were measured (2θ < 60.5°) of which 8365 were unique (R_{int} 0.0509). Refinement against F^2 to $wR2$: 0.1025 (all data), $R1$ (5597 reflections with $I > 2\sigma(I)$) 0.0415, 541 parameters, no restraints; all non-H atoms were anisotropically refined.

X-ray crystallography data for **8** (crystallized by diffusion of hexane into a dichloromethane solution of **8**) were collected at 150 K using silicon 111 monochromated synchrotron radiation. $C_{22}H_{16}N_6O_2$, M = 396.41 g/mol, crystal size 0.08 × 0.04 × 0.01 mm^3, yellow plate, space group $C2/c$, a = 17.6352(9) Å, b = 16.8426(8) Å, c = 6.6854(3) Å, α = 90.00°, β = 107.786(3)°, γ = 90.00°, V = 1890.81(16) $Å^3$, Z = 4, ρ_{calcd} = 1.393 mg/m^3, μ = 0.094 mm^{-1}, 11 539 reflections were measured (2θ < 60.5°) of which 2179 were unique (R_{int} 0.0311). Refinement against F^2 to $wR2$: 0.0997 (all data), $R1$ (1496 reflections with $I > 2\sigma(I)$) 0.0406, 138 parameters, no restraints; all non-H atoms were anisotropically refined.

X-ray crystallography data for **9** (crystallized serendipitously from tetrahydrofuran-d_8 in an NMR tube) were collected at 150 K using graphite-monochromated Mo Kα radiation. $C_{24}H_{12}N_{10} \cdot 2THF$, M = 584.64 g/mol, crystal size 0.40 × 0.35 × 0.22 mm^3, dark red block, space group $C2/c$, a = 9.3164(17) Å, b = 7.0649(13) Å, c = 23.684(4) Å, α = 90.00°, β = 99.945(3)°, γ = 90.00°, V = 1535.4(5) $Å^3$, Z = 4, ρ_{calcd} = 1.438 mg/m^3, μ(Mo Kα) = 0.092 mm^{-1}, 11 372 reflections were measured (2θ < 54.3°) of which 2896 were unique (R_{int} 0.0539). Refinement against F^2 to $wR2$: 0.1237 (all data), $R1$ (1774 reflections with $I > 2\sigma(I)$) 0.0538, 203 parameters, no restraints; all non-H atoms were anisotropic refined.

Acknowledgment. This research was supported by the World Premier International Research Center Initiative (WPI Initiative) on Materials Nanoarchitectonics, by Grant-in-Aid for Scientific Research on Priority Area "Super-Hierarchical Structures" from Ministry of Education, Culture, Sports, Science and Technology, Japan, the National Science Foundation (Grant 0804015 to F.D.) and NSF-EPSCoR programs. We are also grateful to Dr. Akira Sato (NIMS) for X-ray crystallographic data collection on compounds **2** and **9**.

Supporting Information Available: Additional experimental details. Cif files for **2**, **3**, **8**, and **9**. ORTEP diagrams of **2**, **3**, **8**, and **9**. Cartesian coordinates and projections of the calculated structures. This material is available free of charge via the Internet at http://pubs.acs.org.

(32) Sheldrick G. M. *SHELXTL 5.1*; Bruker AXS Inc.: Madison, WI, **1997**.